From an antiferromagnet to a valence bond solid: evidence for a first-order phase transition

J. Stat. Mech. (2008) P02009

(http://iopscience.iop.org/1742-5468/2008/02/P02009)

Journal of Statistical Mechanics: Theory and Experiment
An IOP and SISSA journal

From an antiferromagnet to a valence bond solid: evidence for a first-order phase transition

F-J Jiang[1], M Nyfeler[1], S Chandrasekharan[2] and U-J Wiese[1]

[1] Institute for Theoretical Physics, Bern University, Sidlerstrasse 5, CH-3012 Bern, Switzerland
[2] Department of Physics, Duke University, Box 90305, Durham, NC 27708, USA
E-mail: fjjiang@itp.unibe.ch, nyfeler@itp.unibe.ch, sch@phy.duke.edu and wiese@itp.unibe.ch

Received 2 November 2007
Accepted 23 January 2008
Published 25 February 2008

Online at stacks.iop.org/JSTAT/2008/P02009
doi:10.1088/1742-5468/2008/02/P02009

Abstract. Using a loop–cluster algorithm we investigate the spin-$\frac{1}{2}$ Heisenberg antiferromagnet on a square lattice with exchange coupling J and an additional four-spin interaction of strength Q. We confirm the existence of a phase transition separating antiferromagnetism at $J/Q > J_c/Q$ from a valence bond solid (VBS) state at $J/Q < J_c/Q$. Although our Monte Carlo data are consistent with those of previous studies, we do not confirm the existence of a deconfined quantum critical point. Instead, using a flowgram method on lattices as large as 80^2, we find evidence for a weak first-order phase transition. We also present a detailed study of the antiferromagnetic phase. For $J/Q > J_c/Q$ the staggered magnetization, the spin stiffness and the spinwave velocity of the antiferromagnet are determined by fitting Monte Carlo data to analytic results from the systematic low-energy effective field theory for magnons. Finally, we also investigate the physics of the VBS state at $J/Q < J_c/Q$ and we show that long but finite antiferromagnetic correlations are still present.

Keywords: quantum Monte Carlo simulations, quantum phase transitions (theory)

1742-5468/08/P02009+19$30.00

Contents

1. Introduction

Undoped antiferromagnets, which can be modeled with the spin-$\frac{1}{2}$ Heisenberg Hamiltonian, are among the quantitatively best understood condensed matter systems. Initial numerical evidence that the Heisenberg model has an antiferromagnetically ordered ground state was obtained with a local algorithm on moderate-size lattices in [1]. Very accurate Monte Carlo data on large lattices were obtained with the very efficient loop–cluster algorithm [2]–[4]. The numerical data obtained in this way are in remarkable quantitative agreement with the effective field theory for antiferromagnetic magnons [5]–[9]. In particular, applying chiral perturbation theory—the systematic low-energy effective field theory for Goldstone bosons—to antiferromagnetic magnons, Hasenfratz and Niedermayer [10] have derived analytic expressions for the staggered and uniform susceptibilities. By comparing these expressions with very accurate Monte Carlo data obtained with a loop–cluster algorithm, the staggered magnetization and the spin stiffness, as well as the spinwave velocity of the Heisenberg model, have been determined very precisely [3, 4]. In particular, the resulting values of these low-energy parameters are in quantitative agreement with experimental results on undoped antiferromagnets [11] as well as with results of series expansion around the Ising limit [12]–[14].

High-temperature superconductors result from doping their antiferromagnetic precursor insulators. With increased doping, antiferromagnetism is destroyed before high-temperature superconductivity emerges. Understanding the doped systems from first principles is very difficult because numerical simulations of microscopic systems such

J. Stat. Mech. (2008) P02009

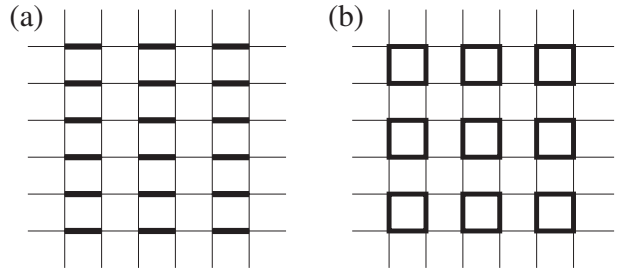

Figure 1. Columnar (a) and plaquette (b) type of VBS order. The solid bonds indicate groups of spins that preferentially form singlets.

J. Stat. Mech. (2008) P02009

as the Hubbard or t–J model suffer from a severe fermion sign problem at a non-zero density of charge carriers. In the cuprates, antiferromagnetism and high-temperature superconductivity are separated by a pseudo-gap regime. It has been conjectured that this regime is connected to a quantum critical point with unusual properties. In particular, the Néel order of the antiferromagnet may give way to a spin liquid phase without long-range magnetic order before the phase coherence of the Cooper pairs of high-temperature superconductivity sets in at somewhat larger doping.

According to the Ginzburg–Landau–Wilson paradigm, a direct phase transition separating one type of order from another should generically be of first order. This paradigm has recently been challenged by the idea of deconfined quantum criticality [15]. A deconfined quantum critical point is a second-order phase transition directly separating two competing ordered phases such as, for example, an antiferromagnet or a superfluid from a valence bond solid (VBS). There are two types for VBS order: columnar and plaquette order, which are illustrated in figure 1. At a deconfined quantum critical point, spinons—i.e. neutral spin-$\frac{1}{2}$ excitations which are confined in the two ordered phases—are liberated and exist as deconfined physical degrees of freedom. It was conjectured that the continuum field theory that describes a deconfined quantum critical point separating an antiferromagnet from a VBS state should be a $(2+1)$-dimensional $\mathbb{C}P(1)$ model with a dynamical non-compact $U(1)$ gage field. This theory is expected to be in the same universality class as an O(3) nonlinear σ model in which the creation or annihilation of baby-Skyrmions is forbidden [16]. The resulting conserved number of baby-Skyrmions gives rise to an additional $U(1)$ symmetry. In [17] it has been argued that—upon doping—a deconfined quantum critical point separating antiferromagnetism from VBS order may extend to a spin liquid phase, thus providing a possible explanation for the pseudo-gap regime in under-doped cuprates.

Establishing the existence of deconfined quantum criticality in an actual physical system is a non-trivial issue. For example, numerical simulations of microscopic models with a transition separating superfluidity from VBS order found a weak first-order transition [18, 19]. Using their flowgram method, in a detailed study of another superfluid–VBS transition Kuklov *et al* have again established a weak first-order transition instead of a quantum critical point [20], thus confirming the Ginzburg–Landau–Wilson paradigm also in that case.

While unbiased numerical simulations of sufficiently strongly doped antiferromagnets are prevented by a severe fermion sign problem, Sandvik has pointed out that there is no

sign problem in the spin-$\frac{1}{2}$ Heisenberg model with a particular four-spin interaction similar to ring exchange [21]. For this model, he presented numerical evidence for a deconfined quantum critical point separating antiferromagnetism from VBS order. The quantum Monte Carlo study of [21] was performed using a projector Monte Carlo method in the valence bond basis [22, 23] and was limited to zero temperature and to moderate volumes, but has the advantage of studying the ground state directly. Recently, Melko and Kaul have simulated the same system on larger lattices at finite temperature using a stochastic series expansion method [24]. Both studies [21, 24] conclude that the transition belongs to a new universality class that is inconsistent with the Ginzburg–Landau–Wilson paradigm. As we will discuss, this conclusion rests on the use of sub-leading corrections to scaling, which can, however, not be determined unambiguously from the data. In this paper, we apply a rather efficient loop–cluster algorithm to the same system. This has allowed us to also reach large volumes. In order to decide if the transition is second or weakly first order, we have implemented the flowgram method of [20]. Our data provide evidence that the transition is weakly first order, i.e. the Ginzburg–Landau–Wilson paradigm is again confirmed. This means that an $SU(2)$ or $U(1)$ invariant system, for which the phenomenon of deconfined quantum criticality can be firmly established, has yet to be found[3]. Finding such a system is non-trivial, in particular, since it should be accessible to accurate first-principles numerical simulations. In this context, it is interesting to consult [25]–[31].

Besides studying the phase transition, we also investigate in detail how antiferromagnetism is weakened. In particular, we extend the results of [3, 4] by determining the staggered magnetization and the spin stiffness, as well as the spinwave velocity of the Heisenberg antiferromagnet, as functions of the strength of the four-spin interaction. In addition, we investigate some properties of the VBS phase.

The rest of this paper is organized as follows. The Heisenberg model with four-spin interactions as well as some relevant observables are introduced in section 2. In section 3 the weakening of antiferromagnetism is studied by comparing Monte Carlo data with analytic predictions from the systematic low-energy effective theory for magnons. In section 4 the phase transition and, in particular, the question of its order is investigated. Some properties of the VBS phase are studied in section 5. Finally, section 6 contains our conclusions.

2. Spin model and observables

In this section we introduce the microscopic Heisenberg Hamiltonian with four-spin interaction, as well as some relevant observables.

2.1. Heisenberg model with four-spin interaction

Let us consider the spin-$\frac{1}{2}$ Heisenberg model on a two-dimensional periodic square lattice of side length L with an additional four-spin interaction defined by the Hamiltonian

$$H = J \sum_{x,i} \vec{S}_x \cdot \vec{S}_{x+\hat{i}} - Q \sum_x \Big[\Big(\vec{S}_x \cdot \vec{S}_{x+\hat{1}} - \tfrac{1}{4} \Big) \Big(\vec{S}_{x+\hat{2}} \cdot \vec{S}_{x+\hat{1}+\hat{2}} - \tfrac{1}{4} \Big) + \Big(\vec{S}_x \cdot \vec{S}_{x+\hat{2}} - \tfrac{1}{4} \Big) \Big(\vec{S}_{x+\hat{1}} \cdot \vec{S}_{x+\hat{1}+\hat{2}} - \tfrac{1}{4} \Big) \Big] . \tag{2.1}$$

[3] Renormalization group arguments have been used to demonstrate the existence of deconfined quantum criticality in an $SU(N)$-invariant system at very large N.

J. Stat. Mech. (2008) P02009

Here $\vec{S}_x = \frac{1}{2}\vec{\sigma}_x$ is a spin-$\frac{1}{2}$ operator located at the lattice site x and $\hat{\imath}$ is a vector of length a (where a is the lattice spacing) pointing in the i-direction. The standard exchange coupling $J > 0$ favors anti-parallel spins. The four-spin coupling $Q > 0$ favors the simultaneous formation of singlet pairs on opposite sides of an elementary plaquette. Sandvik has pointed out that quantum Monte Carlo simulations of this four-spin interaction do not suffer from the sign problem [21]. Indeed, the fact that it can be treated reliably in numerical simulations is the main reason to consider this particular form of the coupling.

2.2. Observables

Obviously, the above Hamiltonian commutes with the uniform magnetization

$$\vec{M} = \sum_x \vec{S}_x. \tag{2.2}$$

The order parameter for antiferromagnetism is the staggered magnetization

$$\vec{M}_{\rm s} = \sum_x (-1)^{(x_1+x_2)/a} \vec{S}_x. \tag{2.3}$$

A physical quantity of central interest is the staggered susceptibility

$$\chi_{\rm s} = \frac{1}{L^2}\int_0^\beta {\rm d}t\, \langle M^3_{\rm s}(0) M^3_{\rm s}(t)\rangle = \frac{1}{L^2}\int_0^\beta {\rm d}t\, \frac{1}{Z}\,{\rm Tr}[M^3_{\rm s}(0) M^3_{\rm s}(t)\exp(-\beta H)], \tag{2.4}$$

the integrated correlation function of the 3-component of the staggered magnetization operator. Here β is the inverse temperature and

$$Z = {\rm Tr}\exp(-\beta H) \tag{2.5}$$

is the partition function. Another relevant quantity is the uniform susceptibility

$$\chi_{\rm u} = \frac{1}{L^2}\int_0^\beta {\rm d}t\, \langle M^3(0) M^3(t)\rangle = \frac{1}{L^2}\int_0^\beta {\rm d}t\, \frac{1}{Z}\,{\rm Tr}[M^3(0) M^3(t)\exp(-\beta H)], \tag{2.6}$$

the integrated correlation function of the uniform magnetization. Both $\chi_{\rm s}$ and $\chi_{\rm u}$ can be measured very efficiently with the loop–cluster algorithm using improved estimators [3]. In particular, in the multi-cluster version of the algorithm the staggered susceptibility

$$\chi_{\rm s} = \frac{1}{4\beta L^2}\left\langle \sum_{\mathcal{C}} |\mathcal{C}|^2 \right\rangle \tag{2.7}$$

is given in terms of the cluster sizes $|\mathcal{C}|$ (which have the dimension of time). Similarly, the uniform susceptibility

$$\chi_{\rm u} = \frac{\beta}{4L^2}\langle W_{\rm t}^2\rangle = \frac{\beta}{4L^2}\left\langle \sum_{\mathcal{C}} W_{\rm t}(\mathcal{C})^2 \right\rangle \tag{2.8}$$

is given in terms of the temporal winding number $W_{\rm t} = \sum_{\mathcal{C}} W_{\rm t}(\mathcal{C})$, which is the sum of winding numbers $W_{\rm t}(\mathcal{C})$ of the loop–clusters $\mathcal{C}$ around the Euclidean time direction. In complete analogy, the spatial winding numbers $W_i = \sum_{\mathcal{C}} W_i(\mathcal{C})$ define

J. Stat. Mech. (2008) P02009

two spatial susceptibilities

$$\chi_i = \frac{1}{4\beta}\left\langle W_i^2 \right\rangle = \frac{1}{4\beta}\left\langle \sum_{\mathcal{C}} W_i(\mathcal{C})^2 \right\rangle . \tag{2.9}$$

These susceptibilities measure the response of the system to a twist in the spatial boundary conditions.

A natural order parameter that signals a VBS state is

$$D_i = \sum_x (-1)^{x_i/a} \vec{S}_x \cdot \vec{S}_{x+\hat{i}}. \tag{2.10}$$

In a VBS state with columnar order either D_1 or D_2 has a non-vanishing vacuum expectation value. In a VBS state with plaquette order, on the other hand, one of the linear combinations $D_1 \pm D_2$ has a non-zero expectation value. In numerical simulations, it is easier to investigate an alternative pair of order parameters which just count the number of spin flips in the configurations contributing to the path integral. We define the order parameter $\widetilde{D}_i$ as the difference between the number of spin flips on nearest-neighbor bonds in the i-direction with an even and an odd value of x_i/a. It should be noted that such flips can be due to both the standard two-spin coupling of strength J and the four-spin coupling of strength Q. The corresponding probability distribution $p(\widetilde{D}_1, \widetilde{D}_2)$ is useful for investigating the nature of the VBS state.

3. Weakening of antiferromagnetism

In this section we investigate the weakening of antiferromagnetism. First, we briefly review some results of the systematic low-energy magnon effective field theory. Then Monte Carlo data obtained with a loop–cluster algorithm are used to determine the values of the low-energy parameters of the effective theory.

3.1. Low-energy effective theory for magnons

The low-energy physics of antiferromagnets is determined by the $SU(2)_{\mathrm{s}}$ spin symmetry which is spontaneously broken down to $U(1)_{\mathrm{s}}$. As a result, there are two massless Goldstone bosons—the antiferromagnetic spin waves or magnons. Chakravarty *et al* [5] were the first to describe the low-energy magnon physics by an effective field theory—the $(2+1)$-d O(3)-invariant nonlinear σ model. In analogy to chiral perturbation theory for the pseudo-Goldstone pions in QCD, a systematic low-energy effective field theory for magnons was developed in [6]–[9]. The staggered magnetization of an antiferromagnet is described by a unit-vector field

$$\vec{e}(x) = (e_1(x), e_2(x), e_3(x)), \qquad \vec{e}(x)^2 = 1, \tag{3.1}$$

in the coset space $SU(2)_{\mathrm{s}}/U(1)_{\mathrm{s}} = S^2$. Here $x = (x_1, x_2, t)$ denotes a point in space–time. To leading order, the Euclidean magnon effective action takes the form

$$S[\vec{e}] = \int \mathrm{d}^2x\, \mathrm{d}t\, \frac{\rho_{\mathrm{s}}}{2}\left(\partial_i \vec{e}\cdot\partial_i \vec{e} + \frac{1}{c^2}\partial_t \vec{e}\cdot\partial_t \vec{e}\right). \tag{3.2}$$

The index $i \in \{1,2\}$ labels the two spatial directions, while the index t refers to the Euclidean time direction. The parameter ρ_{s} is the spin stiffness and c is the spinwave

J. Stat. Mech. (2008) P02009

velocity. At low energies the antiferromagnet has a relativistic spectrum. Hence, by introducing $x_0 = ct$ the action takes the manifestly Lorentz-invariant form

$$S[\vec{e}] = \int \mathrm{d}^2x\, \mathrm{d}x_0\, \frac{\rho_\mathrm{s}}{2c} \partial_\mu \vec{e} \cdot \partial_\mu \vec{e}. \tag{3.3}$$

The ratio $\xi = c/(2\pi\rho_\mathrm{s})$ defines a characteristic length scale which diverges when antiferromagnetism disappears at a second-order phase transition.

Hasenfratz and Niedermayer have performed very detailed calculations of a variety of physical quantities including the next to next to leading 2-loop order of the systematic expansion [10]. For our study their results for finite temperature and finite volume effects of the staggered and uniform susceptibilities are most relevant. Depending on the size L of the quadratic periodic spatial volume and the inverse temperature β, one distinguishes cubical space–time volumes with $L \approx \beta c$ from cylindrical ones with $\beta c \gg L$. The aspect ratio of the space–time box is characterized by

$$l = \left(\frac{\beta c}{L}\right)^{1/3}. \tag{3.4}$$

In the cubical regime the volume and temperature dependence of the staggered magnetization is given by

$$\chi_\mathrm{s} = \frac{\mathcal{M}_\mathrm{s}^2 L^2 \beta}{3} \left\{ 1 + 2\frac{c}{\rho_\mathrm{s} L l}\beta_1(l) + \left(\frac{c}{\rho_\mathrm{s} L l}\right)^2 \left[\beta_1(l)^2 + 3\beta_2(l)\right] + \cdots \right\}, \tag{3.5}$$

where $\mathcal{M}_\mathrm{s}$ is the staggered magnetization density. The uniform susceptibility takes the form

$$\chi_\mathrm{u} = \frac{2\rho_\mathrm{s}}{3c^2} \left\{ 1 + \frac{1}{3}\frac{c}{\rho_\mathrm{s} L l}\widetilde{\beta}_1(l) + \frac{1}{3}\left(\frac{c}{\rho_\mathrm{s} L l}\right)^2 \left[\widetilde{\beta}_2(l) - \frac{1}{3}\widetilde{\beta}_1(l)^2 - 6\psi(l)\right] + \cdots \right\}. \tag{3.6}$$

The functions $\beta_i(l)$, $\widetilde{\beta}_i(l)$, and $\psi(l)$ are shape coefficients of the space–time box defined in [10].

3.2. Determination of the low-energy parameters

We have performed numerical simulations of the Heisenberg model with four-spin interaction for a variety of lattice sizes L/a ranging from 24 to 112 at inverse temperatures between $\beta J = 10$ and 20. Remarkably, just like the ordinary two-spin coupling, the additional four-spin coupling can also be treated with an efficient loop–cluster algorithm. The algorithm, presently implemented only in discrete time, will be described elsewhere. All simulations described in this section have been performed at three different lattice spacings in discrete time, which allows a reliable extrapolation to the continuum limit. Some numerical data (extrapolated to the time-continuum limit) are listed in table 1. For fixed J and Q all data for χ_s and χ_u have been fitted simultaneously to equations (3.5) and (3.6) by using the low-energy constants $\mathcal{M}_\mathrm{s}$, ρ_s and c as fitting parameters. The fits are very good with χ^2/d.o.f. ranging from 0.5 to 2.0. Typical fits are shown in figures 2(a) and (b). The corresponding results are summarized in table 2 and illustrated in figures 3 and 4. One observes a substantial weakening of antiferromagnetism. In

J. Stat. Mech. (2008) P02009

Table 1. Some numerical data for the staggered susceptibility and the temporal winding number squared $\langle W_t^2 \rangle$ obtained with the loop–cluster algorithm.

Q/J	βJ	L/a	$\chi_s Ja$	$\langle W_t^2 \rangle$
0.1	20	34	743.0(1.8)	8.285(26)
0.1	20	36	829(2)	9.312(25)
0.5	16	42	625.1(1.6)	7.561(20)
0.5	16	44	683(2)	8.310(20)
1	12	42	333.7(1.3)	5.361(20)
1	12	46	396.3(1.5)	6.434(22)
2	12	66	470.8(1.6)	5.598(20)
2	12	68	497.7(1.6)	5.960(22)
3	10	78	383.8(1.2)	5.310(21)
3	10	82	420.8(1.2)	5.914(22)
4	10	94	415.9(1.5)	5.011(23)
4	10	96	431.4(1.5)	5.229(26)

Table 2. Results for the low-energy parameters $\mathcal{M}_s$, ρ_s, and c as well as the length scale $\xi = c/(2\pi\rho_s)$ obtained from fitting χ_s and χ_u to the analytic expressions of equations (3.5) and (3.6) from the magnon effective theory.

Q/J	$\mathcal{M}_s a^2$	ρ_s/J	$c/(Ja^2)$	ξ/a
0	0.3074(4)	0.186(4)	1.68(1)	1.44(3)
0.1	0.2909(6)	0.183(6)	1.88(3)	1.64(3)
0.5	0.2383(7)	0.182(6)	2.73(4)	2.39(4)
1	0.1965(7)	0.194(7)	3.90(6)	3.19(5)
2	0.149(1)	0.194(9)	5.98(14)	4.91(12)
3	0.122(1)	0.192(8)	7.97(16)	6.60(14)
4	0.106(1)	0.218(13)	10.50(31)	7.67(26)

particular, as one goes from $Q = 0$ to $4J$, the staggered magnetization $\mathcal{M}_s$ decreases by a factor of about 3, while the correlation length $\xi = c/(2\pi\rho_s)$ increases by a factor of about 5. Interestingly, in units of J, the spin stiffness ρ_s is more or less constant. The increase of ξ with Q is thus due to an increase of the spinwave velocity c (in units of Ja^2). When antiferromagnetism disappears at a second-order phase transition, the correlation length ξ diverges. This is possible only if ρ_s goes to zero at the transition. Since the system interacts locally, any excitation travels with a finite speed, and hence c cannot go to infinity. In the next section we will present numerical evidence for a first-order phase transition. In that case, ρ_s remains finite at the transition.

4. Phase transition between antiferromagnetism and VBS order

In this section we study the phase transition at which antiferromagnetism turns into VBS order. In particular, the order of the transition is investigated using both finite-size scaling and the flowgram method of [20].

J. Stat. Mech. (2008) P02009

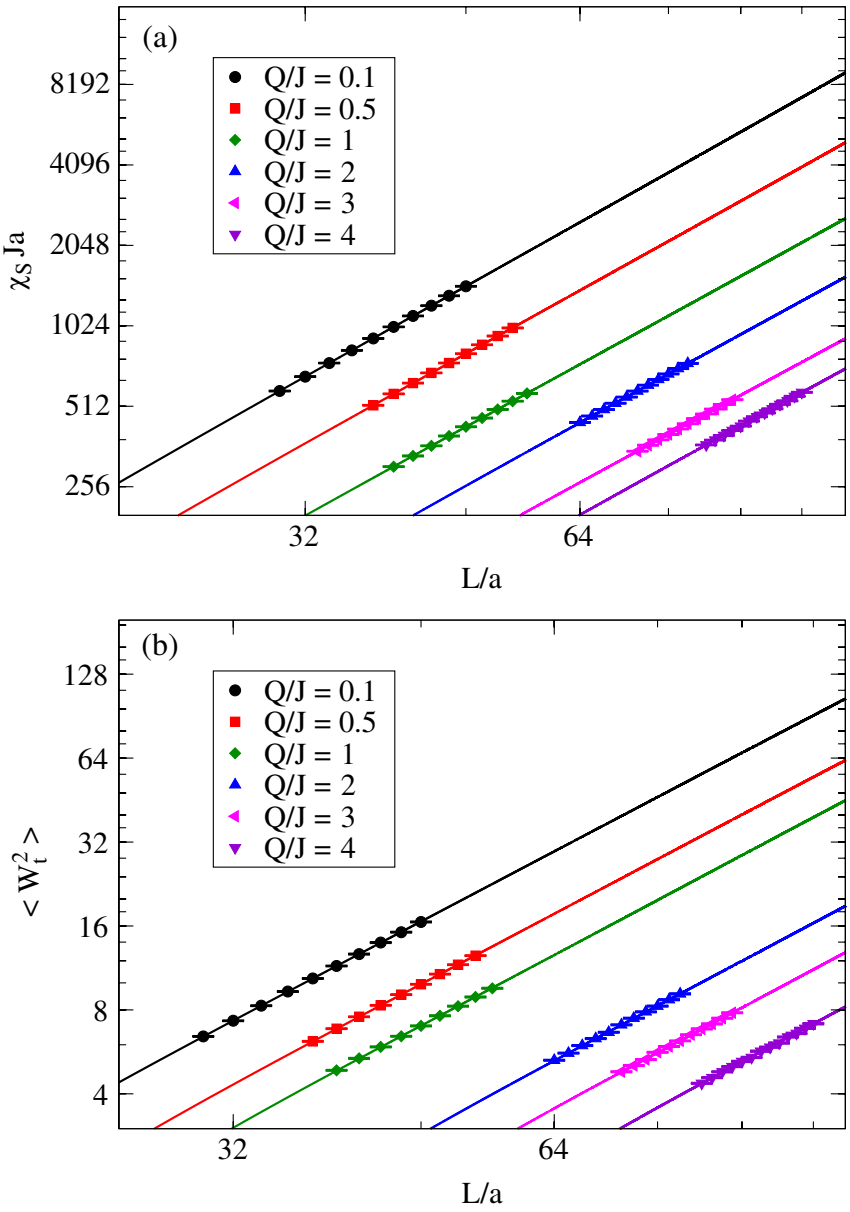

Figure 2. Fit of the finite-size and finite-temperature effects of the staggered susceptibility χ_s (a) and the temporal winding number squared $\langle W_t^2 \rangle$ (b) to results of the effective theory in the cubical regime for various values of Q/J.

4.1. Finite-size effects of $\langle W_i^2 \rangle$ near the transition

As we have seen in the previous section, antiferromagnetism is substantially weakened as the four-spin coupling Q increases. This manifests itself in the reduction of the staggered magnetization $\mathcal{M}_s$ as well as in the increase of the characteristic length scale $\xi = c/(2\pi\rho_s)$. The higher-order terms in the systematic expansion are suppressed as long as $L \gg \xi$. In practice, this limits us to $\xi \approx 10a$ which corresponds to $Q/J \approx 5$. As one approaches a second-order phase transition, ξ diverges and the systematic effective theory is no longer

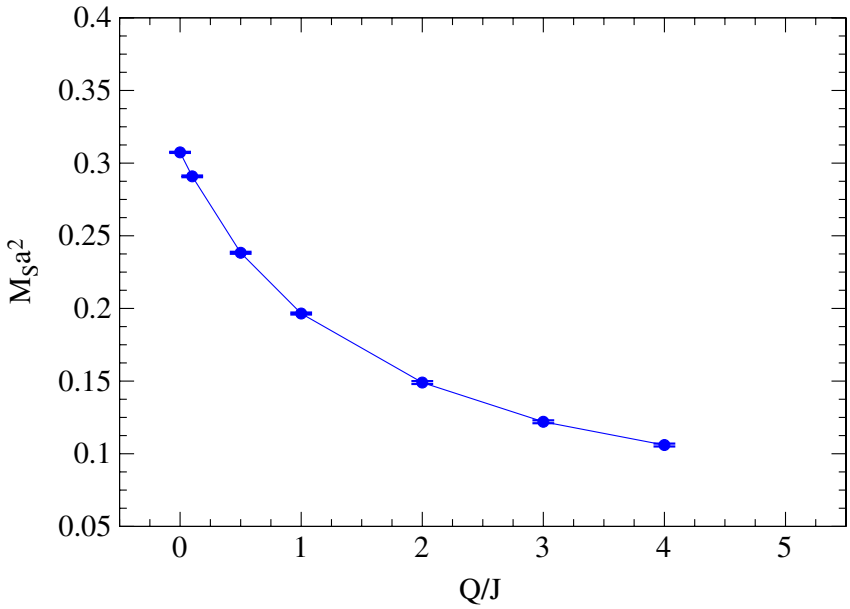

Figure 3. The staggered magnetization $\mathcal{M}_s$ as a function of Q/J, obtained from the fits to the magnon effective theory results for χ_s and χ_u.

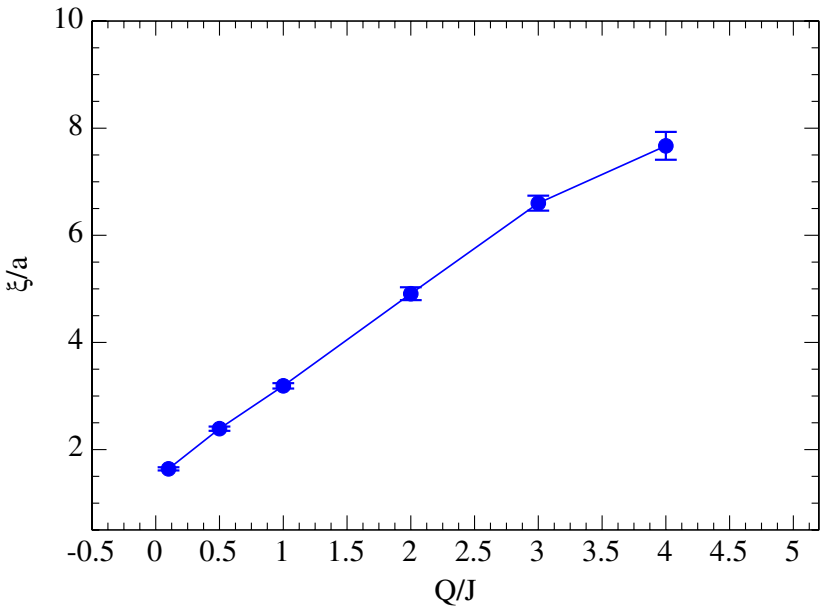

Figure 4. The length scale $\xi = c/(2\pi\rho_s)$ as a function of Q/J, obtained from the fits to the magnon effective theory results for χ_s and χ_u.

applicable. Instead, in the vicinity of the phase transition, it is useful to employ finite-size scaling.

In order to locate the transition it is natural to investigate the J/Q dependence of the spatial winding number squared $\langle W_i^2 \rangle$. In particular, in the case of a second-order phase transition, for sufficiently large volumes the various finite volume curves should all

doi:10.1088/1742-5468/2008/02/P02009

intersect at the critical coupling. Recently, such an analysis has been reported by Melko and Kaul [24]. We have verified explicitly that our Monte Carlo data are consistent with those of that study. In figure 5(a) we show a fit to those data for moderate volumes $L/a = 32, 40$ and 48 near the transition using the finite-size scaling ansatz

$$\langle W_i^2 \rangle = f\left(\frac{J - J_c}{J_c} L^{1/\nu}\right) = A + B\frac{J - J_c}{J_c} L^{1/\nu} + \mathcal{O}\left(\left(\frac{J - J_c}{J_c}\right)^2\right). \quad (4.1)$$

The fit is good, with $\chi^2/\text{d.o.f.} \approx 2$, suggesting that the transition might actually be second order. In particular, the three finite volume curves intersect in one point, $J_c/Q = 0.0375(5)$, and do not require an additive sub-leading correction $CL^{-\omega}$ to equation (4.1). This is consistent with Sandvik's earlier result obtained on smaller volumes $L/a = 16, \ldots, 32$ which did require the inclusion of the sub-leading term. His fit led to $\omega \approx 2$, which implies that the corrections are suppressed for large volumes. Remarkably, when Melko and Kaul's $L/a = 64$ data are included in the fit of equation (4.1), its quality degrades to $\chi^2/\text{d.o.f.} \approx 8$.[4] In fact, the $L/a = 64$ curve does not pass through the intersection point of the smaller volume curves. Melko and Kaul attribute this behavior to sub-leading terms and finally come to the conclusion that there is a deconfined quantum critical point somewhere in the interval $0.038 < J/Q < 0.040$. Indeed, a fit including an additional sub-leading term $CL^{-\omega}$ is possible. However, the exponent ω is not well determined by the data. In order to obtain a stable fit, we have fixed ω to different values ranging from 0.01 to 2.5, which all give more or less the same $\chi^2/\text{d.o.f.} \approx 2.5$, but lead to different values of the critical coupling J_c. For example, fixing $\omega = 2$, as suggested by [21], one obtains $J_c/Q = 0.0404(4)$ and $\nu = 0.62(2)$. This fit is illustrated in figure 5(b). On the other hand, when one fixes $\omega = 0.01$, one obtains $J_c/Q = 0.0438(7)$ and $\nu = 0.62(2)$. Finally, when one excludes all but the largest volumes $L/a = 40, 48$ and 64, a four-parameter fit becomes possible again. This fit, shown in figure 5(c), is less good with $\chi^2/\text{d.o.f.} \approx 3.5$ and it yields $J_c/Q = 0.0398(6)$, which is inconsistent with the critical coupling obtained from the moderate volume data. Even larger volumes would be needed in order to decide if the curves will continue to intersect in the same point.

To summarize, the moderate volume data (with $L/a = 32, 40$ and 48) are well described by the four-parameter fit of equation (4.1), while all data including those for $L/a = 64$ are not. These data can be described by a six-parameter fit including sub-leading corrections, but the data do not unambiguously determine the fitting parameters. Since no sub-leading term is required to fit the moderate volume data, it seems strange that such corrections become necessary once larger volumes are included in the fit. We take this unusual behavior as a first indication that the transition may actually be weakly first order.

Another observation that may cast some doubt on the second-order nature of the transition is a non-monotonic behavior of $\langle W_i^2 \rangle$ near the transition, which is displayed in figure 6. Such behavior is typical for a first-order phase transition. For example, in the VBS phase, at a point close to a first-order transition, domains of antiferromagnetic phase can still exist. Thus, for small volumes, the antiferromagnetic domains may lead to a linear increase of $\langle W_i^2 \rangle$ with L. For larger volumes, the VBS phase will begin to dominate

[4] Even if one excludes by hand the somewhat suspicious data point at $L/a = 64$ and $J/Q = 0.038$, which may be due to an unusually large statistical fluctuation, the quality of the fit still degrades to $\chi^2/\text{d.o.f.} \approx 6$.

J. Stat. Mech. (2008) P02009

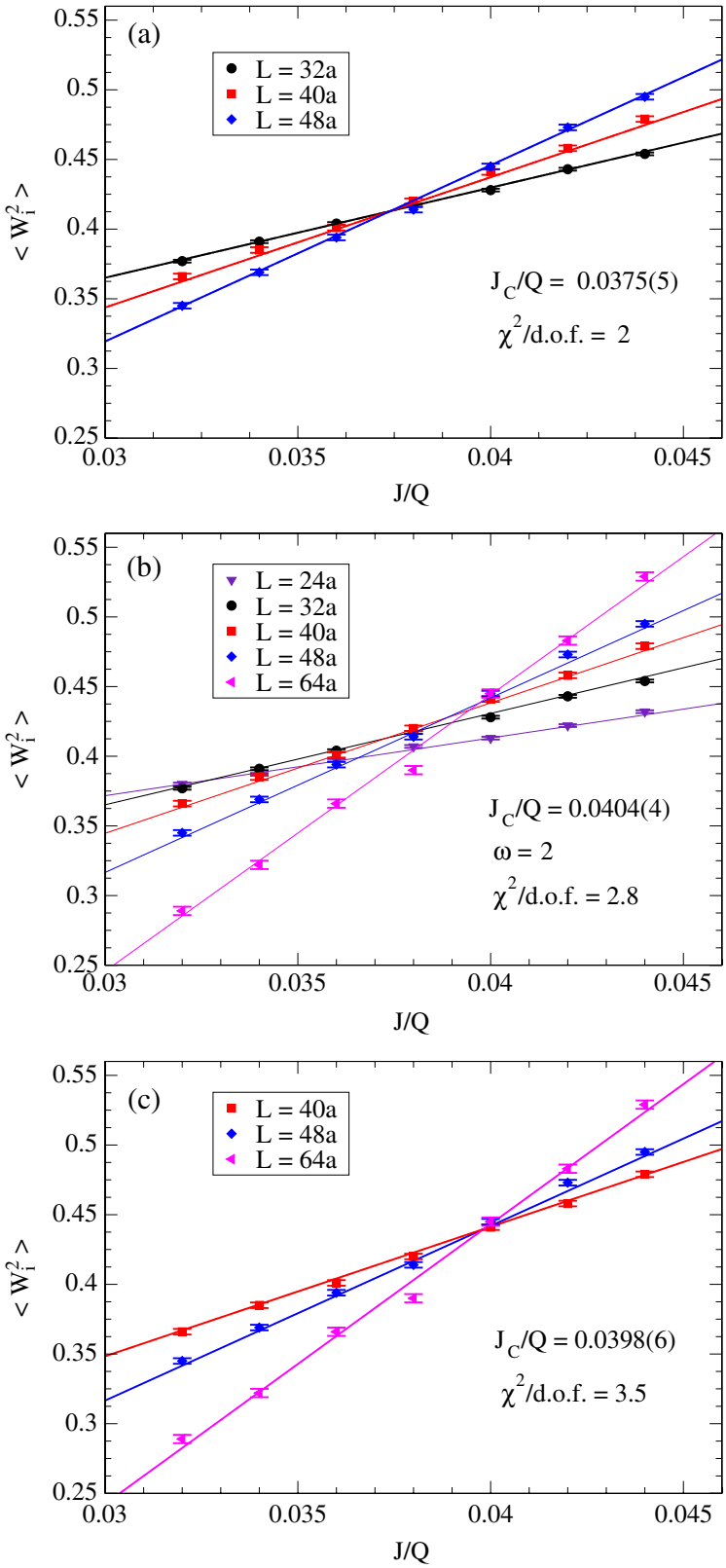

Figure 5. Three different fits of the spatial winding number squared $\langle W_i^2 \rangle$ as a function of the coupling J/Q in the transition region.

J. Stat. Mech. (2008) P02009

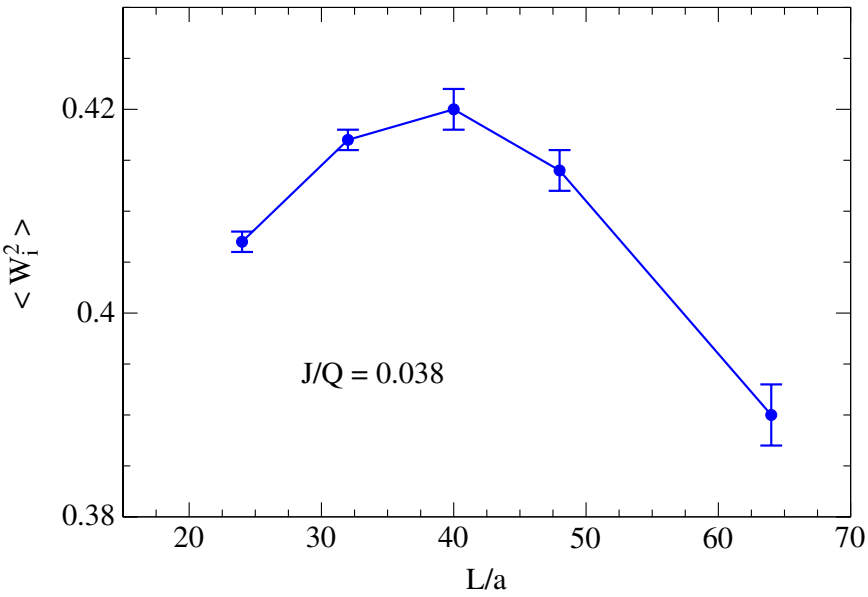

Figure 6. Non-monotonic volume dependence of $\langle W_i^2 \rangle$ at $J/Q = 0.038$ near the critical coupling that may indicate a weak first-order phase transition.

and $\langle W_i^2 \rangle$ will then decrease. This competition can lead to non-monotonic behavior. For these reasons, we think that the data of [21] and [24] do not provide sufficiently convincing evidence that deconfined quantum criticality has actually been observed. Due to limited numerical resources, we have not been able to extend the analysis to substantially larger volumes. However, using a supercomputer this would definitely be possible and, in fact, highly desirable. In order to shed more light on the subtle issue of quantum criticality versus a weak first-order transition, we now turn to an alternative method of analysis.

4.2. Application of the flowgram method

Kuklov *et al* have developed a flowgram method which is useful for distinguishing weakly first-order from second-order phase transitions [20]. For our system, the flowgram method can be implemented as follows. We work on lattices of increasing size L at the inverse temperature given by $\beta Q = L/a$. First, each individual spin configuration in the path integral is associated with either the antiferromagnetic or the VBS phase according to the following criterion. If all three winding numbers W_1, W_2 and W_t are equal to zero, the configuration is associated with the VBS phase. On the other hand, if at least one of the three winding numbers is non-zero, the configuration is associated with the antiferromagnetic phase. This criterion is natural, because in the infinite volume limit there is no winding in the VBS phase, while there is always some winding in the antiferromagnetic phase. One then defines a volume-dependent pseudo-critical coupling $J_c(L)$ at which both competing phases have equal weight, i.e. the number of associated configurations is the same for both phases. It is important to note that, in the infinite volume limit, the pseudo-critical coupling $J_c(L)$ approaches the true location of the phase transition both for a first- and for a second-order phase transition. The large volume limit is now approached by simulating systems at the pseudo-critical coupling $J_c(L)$ for

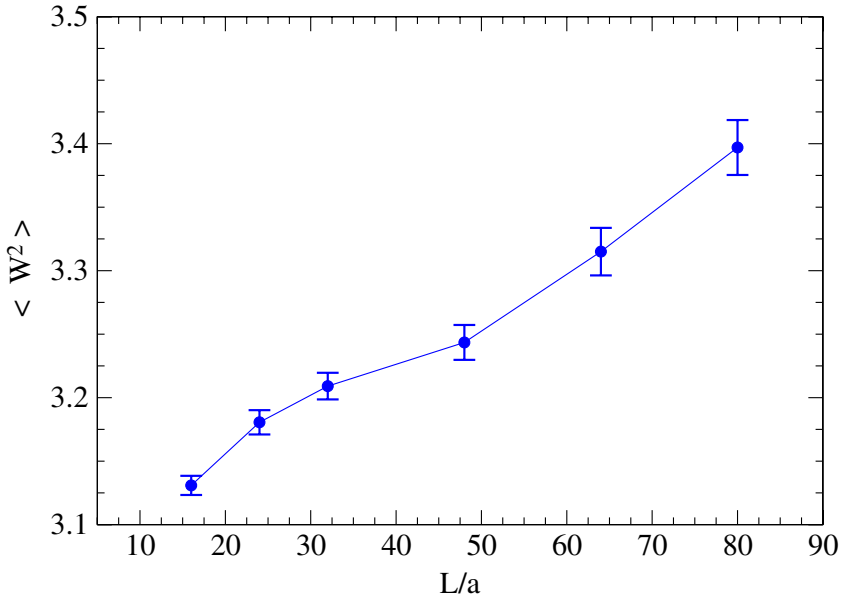

Figure 7. The sum of spatial and temporal winding numbers squared $\langle W^2\rangle(J_c(L))$ evaluated at the pseudo-critical coupling $J_c(L)$ for increasing lattice size L.

increasing values of L. Defining the sum of the spatial and temporal winding numbers squared as $W^2 = W_1^2+W_2^2+W_t^2$, the quantity $\langle W^2\rangle(J_c(L))$ is then evaluated at the pseudo-critical coupling $J_c(L)$. If the phase transition is second order, $\langle W^2\rangle(J_c(L))$ will approach a constant for large L since ρ_s then vanishes (i.e. $\xi = c/(2\pi\rho_s)$ diverges) at the transition. On the other hand, if the transition is first order, with 50% probability the system still shows the characteristics of the antiferromagnet. Thus, for $L \gg \xi$, $\langle W^2\rangle(J_c(L))$ grows linearly with L. As we will see below, for $48a \leq L \leq 80a$ we indeed observe this behavior.

We have implemented the Ferrenberg–Swendsen re-weighting method [32] in order to accurately locate the pseudo-critical coupling. Unlike in the rest of this paper, the simulations in this subsection have only been performed at two (instead of three) lattice spacings in discrete time. Both lattice spacings are close to the continuum limit and give consistent results. Instead of extrapolating to the continuum limit (which is less reliable with two than with three lattice spacings), in this subsection we quote our results at the smaller lattice spacing $\varepsilon Q = 0.05$. A calculation closer to the continuum limit or, even better, using a continuous-time algorithm would still be useful.

In order to investigate whether the phase transition is second or weakly first order, the values of $\langle W^2\rangle$ at the pseudo-critical coupling $J_c(L)$ are illustrated in figure 7. For moderate volumes up to $L = 48a$ the curve seems to level off, which would be characteristic of a second-order phase transition. Indeed, as we have seen before, the moderate volume data for the spatial susceptibility are consistent with the finite-size scaling behavior of a second-order phase transition. However, for larger volumes the curve rises linearly, thus indicating a weak first-order phase transition. Of course, one cannot completely exclude that the curve may eventually level off at even larger volumes. For the future, it would be very welcome to generate larger volume data (preferably with a continuous-

J. Stat. Mech. (2008) P02009

Table 3. Values of the volume-dependent pseudo-critical couplings $J_c(L)$ and $J'_c(L)$ obtained with the Ferrenberg–Swendsen re-weighting method.

L/a	24	32	48	64	80	96
$J_c(L)/Q$	0.0311(4)	0.0316(3)	0.0337(4)	0.0364(3)	0.0384(3)	—
$J'_c(L)/Q$	0.115(2)	0.0871(4)	0.0632(4)	0.0544(5)	0.0477(4)	0.0446(4)

time algorithm) in order to rule out this possibility with even higher confidence. We find the leveling-off scenario unlikely and conclude that our results cast serious doubt on the picture of deconfined quantum criticality painted in the earlier studies.

Given the evidence for a weak first-order transition, we like to determine the value of the critical coupling J_c in the infinite volume. The values of the pseudo-critical coupling $J_c(L)$ in a finite volume are summarized in table 3. Given the data for $J_c(L)$ alone, it is non-trivial to extract the infinite volume critical coupling $J_c = J_c(L \to \infty)$. For this reason, we have defined another pseudo-critical coupling $J'_c(L)$, which also extrapolates to the correct limit, i.e. $J'_c(L \to \infty) = J_c$. In this case, we work at the inverse temperature given by $\beta Q = L/4a$. Irrespective of the spatial winding numbers, if the temporal winding number W_t is equal to zero, the configuration is now associated with the VBS phase. On the other hand, if W_t is non-zero, the configuration is associated with the antiferromagnetic phase. As before, we define the volume-dependent pseudo-critical coupling $J'_c(L)$ such that both phases have equal weight. The values of $J'_c(L)$ (again quoted at $\varepsilon Q = 0.05$) are also listed in table 3. According to the finite-size scaling theory for first-order phase transitions, using $\beta L^2 \propto L^3$, both finite volume pseudo-critical couplings should approach their common infinite volume limit J_c as

$$J_c(L) = J_c + C\frac{\log L/a}{L^3}, \qquad J'_c(L) = J_c + C'\frac{\log L/a}{L^3}. \tag{4.2}$$

Interestingly, the two pseudo-critical couplings indeed converge to the same limit. A fit of $J_c(L)$ and $J'_c(L)$ to equation (4.2)—shown in figure 8—has $\chi^2/\text{d.o.f.} \approx 1.2$ and yields the infinite volume critical coupling $J_c = 0.0397(7)$. This is consistent with the assumption that the transition is weakly first order. Again, only the large volume data show the characteristic behavior of a first-order phase transition. It should be noted that the definition of $J'_c(L)$ is less natural than the one of $J_c(L)$, because it ignores the spatial winding numbers when configurations are associated with either of the two phases. In particular, $J'_c(L)$ approaches the infinite volume critical point J_c more slowly than $J_c(L)$. Consequently, the ultimate large volume physics is more easily visible using the pseudo-critical coupling $J_c(L)$. For example, the linear increase of $\langle W^2\rangle(J_c(L))$ with L, which sets in around $L \approx 50a$, is not yet present in $\langle W^2\rangle(J'_c(L))$, and is expected to set in only on larger volumes. Again, for the future, it would be comforting to add data on even larger volumes closer to the transition in order to confirm that the first-order behavior of equation (4.2) persists.

5. Investigation of the VBS state

As we have seen, the antiferromagnet is weakened and ultimately destroyed at a rather weak first-order phase transition. Since the transition is so weak, at moderate volumes it

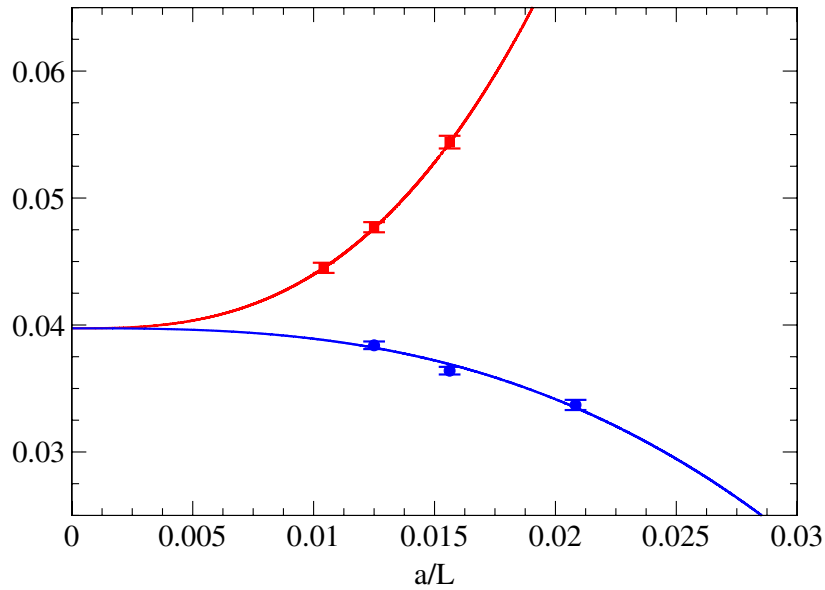

Figure 8. Fit of the pseudo-critical couplings $J_c(L)$ (lower curve) and $J_c'(L)$ (upper curve) shown as functions of a/L.

is practically indistinguishable from a continuous transition. As a result, an approximate $U(1)$ symmetry emerges dynamically as an enhancement of the discrete 90° rotations of the square lattice. The other side of the phase transition is characterized by VBS order. However, the emergent $U(1)$ symmetry makes it difficult to identify the nature of the VBS state as columnar or plaquette.

5.1. Probability distribution of the VBS order parameter

In order to investigate the nature of the VBS order it is best to go away from the critical point as far as possible (assuming that no other phase transitions take place). In the following we thus work at $Q/J = \infty$, which is obtained by putting $J = 0$. The corresponding probability distribution of the standard VBS order parameters $p(D_1, D_2)$ has been determined by Sandvik for a 32^2 lattice at zero temperature and it shows perfect $U(1)$ symmetry [21]. The loop–cluster algorithm allows us to repeat this study for larger volumes, in this case using the probability distribution of the non-standard VBS order parameters $p(\widetilde{D}_1, \widetilde{D}_2)$. As one sees from figure 9, even on a 96^2 lattice at $\beta Q = 30$ one does not see any deviation from the $U(1)$ symmetry. Hence, our data do not allow us to identify the nature of the VBS order. Interestingly, the $U(1)$ symmetry was predicted by the ideas behind deconfined quantum criticality [15]. It is remarkable that this prediction is verified by our data even deep inside the VBS phase, despite the fact that the phase transition is first order. This shows that very long (but not infinite) correlation is indeed generated. Hence, despite our evidence for a weakly first order transition, the observed $U(1)$ symmetry may indicate the possible proximity to a deconfined quantum critical regime. It remains challenging to find a model in which one can show unambiguously and from first principles that this regime actually exists.

J. Stat. Mech. (2008) P02009

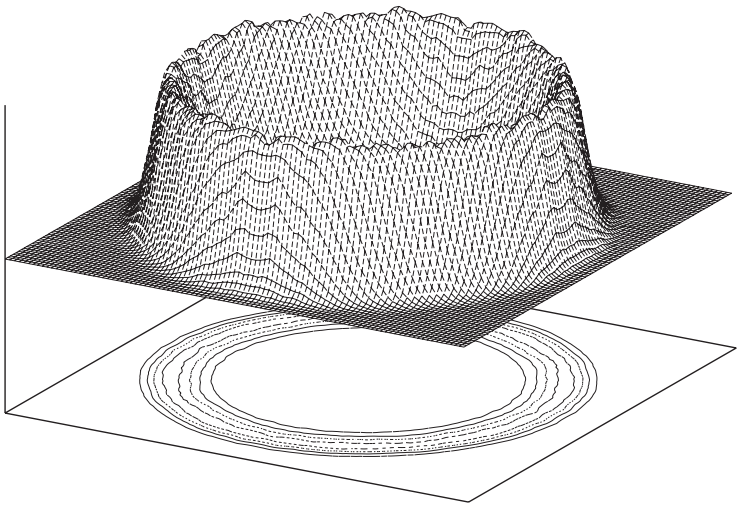

Figure 9. Probability distribution $p(\widetilde{D}_1, \widetilde{D}_2)$ obtained on a 96^2 lattice at $\beta Q = 30$ and $Q/J = \infty$. The observed $U(1)$ rotation symmetry implies that we cannot identify the nature of the VBS phase as either columnar or plaquette.

At small Q/J, the loop cluster algorithm is extremely efficient with auto-correlations limited to at most a few sweeps. However, at larger values of Q/J, and especially at $Q/J = \infty$, the algorithm suffers from a noticeable auto-correlation problem. This problem arises because the cluster algorithm, which is designed to update long-range spin correlations, cannot efficiently shuffle spin-flip events from even to odd bonds. This causes slowing down in the VBS phase. Details concerning the algorithm and its performance will be discussed elsewhere.

5.2. Antiferromagnetic correlations in the VBS phase

In order to confirm that antiferromagnetism indeed disappears for large Q, we again consider $Q/J = \infty$. We have simulated the staggered susceptibility as a function of the lattice size L. As one sees in figure 10, at $\beta Q = 50$ the staggered susceptibility χ_s increases with increasing space–time volume until it levels off around $L \approx 50a$. This shows that long (but not infinite) range antiferromagnetic correlations survive even deep in the VBS phase. These data confirm that antiferromagnetism is indeed destroyed in the VBS phase. However, again one needs to go to volumes larger than $L \approx 50a$ in order to see the ultimate infinite volume behavior.

6. Conclusions

We have employed a rather efficient loop–cluster algorithm to investigate the physics of the antiferromagnetic spin-$\frac{1}{2}$ Heisenberg model with an additional four-spin interaction. When the four-spin coupling is sufficiently strong, antiferromagnetism is destroyed and gives way to a VBS state. While Sandvik's pioneering study [21] was limited to zero temperature and moderate volumes but has the advantage of studying the ground state directly, just like the stochastic series expansion method of Melko and Kaul [24], the cluster algorithm allows us to work at non-zero temperatures and large volumes. Using the cluster

J. Stat. Mech. (2008) P02009

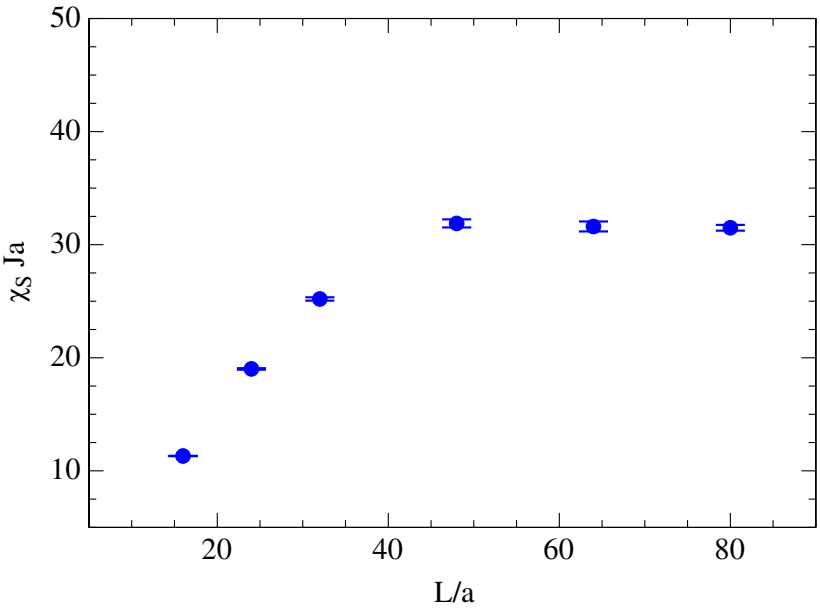

Figure 10. The staggered susceptibility χ_s in the VBS phase increases with increasing space–time volume until it levels off around $L/a \approx 50$ for $\beta Q = 50$.

algorithm and applying the flowgram method of Kuklov *et al* [20], we found numerical evidence for a weak first-order phase transition, thus supporting the Ginzburg–Landau–Wilson paradigm. For the future, it would be comforting to perform numerical simulations on even larger volumes (preferably with a continuous-time algorithm) in order to confirm that the first-order nature of the transition persists. Interestingly, the Ginzburg–Landau–Wilson paradigm was also confirmed in studies of the transition separating superfluidity from VBS order [18]–[20]. The first-order nature of the phase transition in the Heisenberg model with four-spin coupling Q implies that the idea of deconfined quantum criticality again lacks a physical system for which it is firmly established. Hence, the proponents of this intriguing idea are challenged once more to suggest another microscopic system for which one expects this fascinating phenomenon to occur.

It is interesting to ask why the phase transition separating antiferromagnetism from VBS order is so weakly first order. There must be a reason for the long correlation length, around $50a$, even if it does not go to infinity. Also the remarkable $U(1)$ symmetry even deep in the VBS phase needs to be understood. Perhaps, the ideas behind deconfined quantum criticality may still explain these intriguing phenomena.

Acknowledgments

We have benefited from discussions with F Niedermayer and M Troyer. The work of SC was supported in part by the National Science Foundation under grant no. DMR-0506953. We also acknowledge the support of the Schweizerischer Nationalfonds.

References

[1] Reger J D and Young A P, 1988 *Phys. Rev.* B **37** 5978
[2] Evertz H G, Lana G and Marcu M, 1993 *Phys. Rev. Lett.* **70** 875

J. Stat. Mech. (2008) P02009

[3] Wiese U-J and Ying H-P, 1994 *Z. Phys.* B **93** 147
[4] Beard B B and Wiese U-J, 1996 *Phys. Rev. Lett.* **77** 5130
[5] Chakravarty S, Halperin B I and Nelson D R, 1989 *Phys. Rev.* B **39** 2344
[6] Neuberger H and Ziman T, 1989 *Phys. Rev.* B **39** 2608
[7] Fisher D S, 1989 *Phys. Rev.* B **39** 11783
[8] Hasenfratz P and Leutwyler H, 1990 *Nucl. Phys.* B **343** 241
[9] Hasenfratz P and Niedermayer F, 1991 *Phys. Lett.* B **268** 231
[10] Hasenfratz P and Niedermayer F, 1993 *Z. Phys.* B **92** 91
[11] Greven M *et al*, 1994 *Phys. Rev. Lett.* **72** 1096
Greven M *et al*, 1995 *Z. Phys.* B **96** 465
[12] Singh R R P, 1989 *Phys. Rev.* B **39** 9760
[13] Singh R R P and Huse D A, 1989 *Phys. Rev.* B **40** 7247
[14] Zheng W, Oitmaa J and Hamer C J, 1991 *Phys. Rev.* B **43** 8321
[15] Sentil T, Vishwanath A, Balents L, Sachdev S and Fisher M P A, 2004 *Science* **303** 1490
Sentil T, Vishwanath A, Balents L, Sachdev S and Fisher M P A, 2004 *Phys. Rev.* B **70** 144407
[16] Motrunich O and Vishwanath A, 2004 *Phys. Rev.* B **70** 075104
[17] Kaul R K, Kolezhuk A, Levin M, Sachdev S and Senthil T, 2007 *Phys. Rev.* B **75** 235122
[18] Melko R G, Sandvik A W and Scalapino D J, 2004 *Phys. Rev.* B **69** 100408(R)
[19] Kuklov A, Prokof'ev N and Svistunov B, 2004 *Phys. Rev. Lett.* **93** 230402
[20] Kuklov A, Prokof'ev N, Svistunov B and Troyer M, 2006 *Ann. Phys., NY* **321** 1602
[21] Sandvik A W, 2007 *Phys. Rev. Lett.* **98** 227202
[22] Sandvik A W, 2005 *Phys. Rev. Lett.* **95** 207203
[23] Sandvik A W and Beach K S D, 2007 *Preprint* 0704.1469
[24] Melko R G and Kaul R K, 2008 *Phys. Rev. Lett.* **100** 017203
[25] Batista C D and Trugman S A, 2004 *Phys. Rev. Lett.* **93** 217202
[26] Krüger F and Scheidl S, 2006 *Europhys. Lett.* **74** 896
[27] Kragset S, Smorgrav E, Hove J, Nogueira F S and Sudbo A, 2006 *Phys. Rev. Lett.* **97** 247201
[28] Spanu L, Becca F and Sorella S, 2006 *Phys. Rev.* B **73** 134429
[29] Nussinov Z, Batista C D, Normand B and Trugman S A, 2007 *Phys. Rev.* B **75** 094411
[30] Harada K, Kawashima N and Troyer M, 2007 *J. Phys. Soc. Japan* **76** 013703
[31] Grover T and Senthil T, 2007 *Phys. Rev. Lett.* **98** 247202
[32] Ferrenberg A M and Swendsen R H, 1988 *Phys. Rev. Lett.* **61** 2635

J. Stat. Mech. (2008) P02009